THE JOURNAL OF PHYSICAL CHEMISTRY Letters

ACS EDITORS' CHOICE

pubs.acs.org/JPCL

Perspective

Manipulating Electronic Structure from the Bottom-Up: Colloidal Nanocrystal-Based Semiconductors

Sebastian Volk, Nuri Yazdani, and Vanessa Wood*

Cite This: J. Phys. Chem. Lett. 2020, 11, 9255−9264

Read Online

ACCESS | Metrics & More | Article Recommendations

ABSTRACT: Semiconductors assembled from colloidal nanocrystals (NCs) are often described in the same terms as their single-crystalline counterparts with references to conduction and valence band edges, doping densities, and electronic defects; however, how and why semiconductor properties manifest in these bottom-up fabricated thin films can be fundamentally different. In this Perspective, we describe the factors that determine the electronic structure in colloidal NC-based semiconductors, and comment on approaches for measuring or calculating this electronic structure. Finally, we discuss future directions for these semiconductors and highlight their potential to bridge the divide between localized quantum effects and long-range transport in thin films.

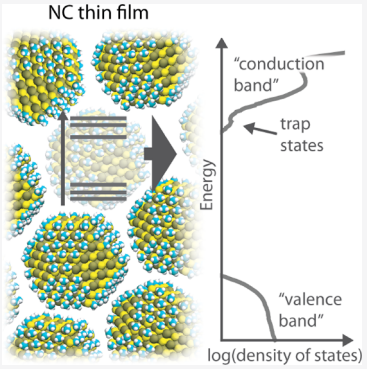

Understanding and controlling the electronic structure in nanocrystal (NC) thin films is imperative for integrating them efficiently into (opto)electronic devices. The past decade of research and development has shown that thin films of NCs can be incorporated into devices as semiconductors, having transport occurring across a well-defined mobility gap[1−3] with n- or p-type behavior.[4−7] While electronic characterization of NC thin films shows similarities to bulk semiconductors, studies of the electronic structure of NC thin films reveal that the origins of doping, free carrier generation, and carrier trapping and recombination in NC thin films are fundamentally different than in bulk semiconductors. In this Perspective, we discuss methods for measuring and understanding the electronic structure of NC thin films as well as the challenges and opportunities for controlling their electronic structure that do not exist in bulk semiconductors.

In selecting a semiconductor for an application, one considers its electronic structure: its band gap, the position of its conduction and valence band, its doping density, the energetic depth of the dopants, and the number density and characteristics of its defect states (e.g., their energetic depths, electron and hole capture coefficients, *etc.*). While individual NCs afford a high degree of tunability with novel properties stemming for example from the quantum-confinement of the constituent NCs (e.g., a size-dependent band gap), to truly leverage the promise NC thin films hold as engineered semiconductors it will be necessary to have understanding and control over standard semiconducting properties.

The electronic structure of an NC thin film is related to the electronic structure of the constituent NCs, and the electronic properties of the individual NCs are determined by their size, composition, shape, and surface.[1−3,8,9] NCs of identical size, shape, composition, and surface assembled into a thin film will form an isoenergetic "conduction band" and "valence band" stemming from the lowest unoccupied electronic states and the highest occupied electronic states of the individual NCs. If the NCs have a finite size distribution, and therefore a distribution in the band gaps of the individual NCs, one measures a "band structure" with an Urbach tail feature.[10] Here "band" is expressed in quotation marks because it is important to keep in mind that the effective band measured in NC thin films in fact stems from a spatial distribution of electronic levels on the individual NCs and not from the bonding of individual atomic orbitals with resulting plane wave electronic extending throughout the NC thin film as in bulk semiconductors. In this sense, NC thin films are in many ways like molecular semiconductors, but with large NC "molecules".

The band gap of individual NCs is primarily defined by its chemical composition and its size (Figure 1). While size has long been used as a way to tune the NC band gap to a desired value, recent years have seen the emergence of ternary and quaternary NCs, where varying cation or anion ratios (e.g., I−III−VI[11−13] or lead halide perovskites[14]) adds another dimension of control to band gap tunability. Furthermore,

Received: May 9, 2020
Accepted: September 15, 2020
Published: September 15, 2020

https://dx.doi.org/10.1021/acs.jpclett.0c01417
J. Phys. Chem. Lett. 2020, 11, 9255−9264

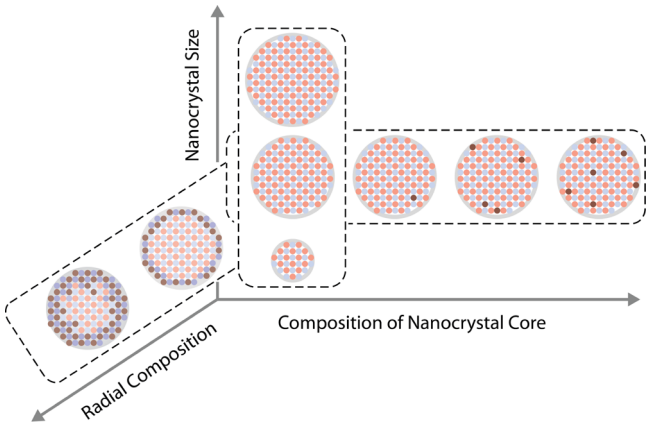

Figure 1. Controlling nanocrystal (NC) band gap. The amount of quantum confinement is defined by both the NC composition and its radius. Radial compositional gradients and core−shell structures can be used to vary the degree of quantum confinement, and the use of ternary or quaternary semiconductors for the NC core offer further tunability beyond that of binary systems.

shells or radial composition gradients can be used to change the carrier confinement in the NC core and therefore the band gap.[15]

Significant shifts (in the meV−eV range) in the position of the energy levels of an NC relative to vacuum can be achieved by (i) changing the surface termination of the NCs[16−19] or (ii) positioning the NC(s) near an interface that causes charge transfer to/from the NC(s).[20] For example, the valence and conduction band onsets of a PbS NC thin film shift up to 1−2 eV because of different surface terminations,[16−19] an effect which stems from the sum of (i) the intrinsic molecular dipole of the terminating ligand and (ii) the surface dipole of the ligand-NC interface (Figure 2).[17] Furthermore, when NCs are placed next to a metallic layer, Fermi level equilibration occurs, leading to interface dipoles formed across individual NCs. These induced vacuum level shifts can be estimated as $\Delta E_{vac} = \frac{|p|}{\varepsilon_0 \varepsilon_r A_{NC}}$, where $|p| = qr$ is the magnitude of the induced surface dipole (with q being the charge lost or gained per NC to achieve Fermi level equilibration and r the radius of the NC), A_{NC} the effective area occupied by an NC, ε_0 the permittivity of free space, and ε_r the relative permittivity of the NC thin-film, which consists of both the NC and the ligands.[20] Accounting for interface dipoles is crucial for accurate device simulation.[21]

The doping of an individual NC depends on its stoichiometry, the ligands, and the presence of impurities and can be determined according to the oxidation-number sum rule:[4,22]

$$N_C V_C + N_A V_A + N_L V_L + \sum_i V_i = \begin{cases} 0, & \text{intrinsic} \\ <0, & \text{p-doped} \\ >0, & \text{n-doped} \end{cases} \quad (2)$$

where N_x and V_x are the number and oxidation states of the cations (C), anions (A), and ligands (L) and V_i is the oxidation state of each impurity (i). Equation 2 shows that doping of an NC semiconductor can occur via (i) heterovalent impurity doping, analogously to bulk semiconductors, or (ii) variation in the stoichiometry and ligand density (Figure 3).

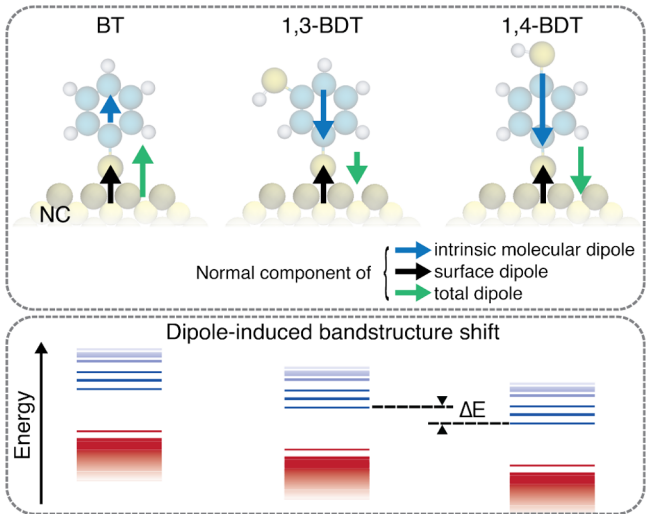

Figure 2. Controlling energy levels of the electronic structure through nanocrystal surface engineering. Top: schematic of a PbS NC surface with different molecular terminations (BT = Benzenethiol; 1,3-BDT = 1,3-Benzenedithiol; 1,4-BDT = 1,4-Benzenedithiol) and their influence on electronic structure (bottom). The sum (green) of the surface dipole (black) and the intrinsic dipole (blue) defines the absolute energy position of valence band (red) and conduction band (blue). Larger net surface dipoles pointing toward the surface result in a shift of the electronic structure toward negative values.[17] For simplicity, only the perpendicular contribution of the surface dipole is depicted in the graphic. Magnitude of dipoles and associated shifts of the electronic structure are not to scale.

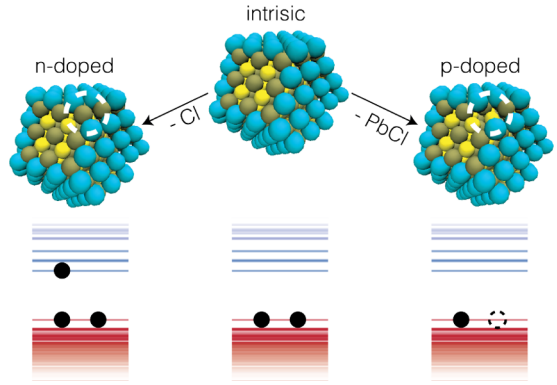

Figure 3. Fermi level modification in NC solids. Stoichiometry changes can be achieved through surface treatments, as in the example of chalcogen and lead enrichment strategies proposed by Oh et al.,[128] resulting in n- and p-type PbSe NCs.

Heterovalent impurity doping can be achieved in NCs during their initial synthesis through proper balancing of the dopant and host precursor kinetics as well as via postsynthesis cation-exchange reactions.[23,24]

Alternatively, NCs can be doped in the absence of impurities by adapting the synthesis and/or postprocessing of the NC-semiconductor so as to achieve n- or p-doped NCs, resulting in charge imbalance among the cation, anion, and ligand species.[25] For example, NCs can be nonstoichiometric as a result of cation- or anion-rich facets terminating the NC.[26] Postsynthetic conditions can also be used to achieve finite doping concentrations, for example via cation/anion exchange reactions[27] and through ligand exchanges.[28]

https://dx.doi.org/10.1021/acs.jpclett.0c01417
J. Phys. Chem. Lett. 2020, 11, 9255−9264

The number of free carriers generated based on NC doping is generally low.[29,30] For example, Bi-doped PbS has reported electron donor densities of around 10^{17} cm^{-3}.[31] These limited doping efficiencies have been attributed to (i) the large ionization energies associated with deep-level impurity states,[31,32] (ii) the charge compensation through surface ligands,[30] and (iii) the dynamic equilibrium of nonionized surface-impurity atoms to core-integrated impurities, as recently reviewed by Kagan.[29]

An emerging alternative doping strategy, which circumvents these possible limitations is that of substitutional doping,[33,34] where remote doping is achieved through the addition of metal NCs within the NC solid.

Electronic midgap states have been identified in NC thin films[35−37] and are detrimental to device performance, decreasing the effective carrier mobility and serving as recombination centers.[38,39]

In analogy to bulk semiconductors, trap states were traditionally associated with deep-level electronic states within the band gap of the individual NCs (Figure 4i).[40] In specific cases, surface defects such as additional, missing, or uncoordinated surface atoms can contribute to electronic midgap states in individual NCs.[41−45] However, computational studies have shown that even nonstoichiometric NCs generally tend to exhibit defect-free band gaps.[46]

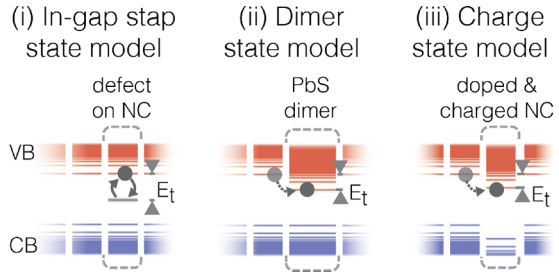

Figure 4. Understanding the origin of electronic trap state formation. Electronic trap states in the band gap of NC semiconductors can form because of (i) in-gap states on individual NCs, (ii) NC dimers (i.e., necked NCs), and (iii) charged, doped NCs. In contrast to the highly localized trap forming because of a defect on an individual NC, when a trap state comes from a charged, doped-NC or from the NC-dimer, the entire NC (or NC dimer) acts as the trap state. Reproduced from ref 47. Copyright 2019 American Chemical Society.

Two other origins for deep trap state formation have been identified and experimentally demonstrated and can occur simultaneously in the same NC thin film.[47] First, deep-level states emerge because of the presence of NC dimers (i.e., necked NCs),[48] a surface and fabrication-step-dependent phenomenon of solution-dispersed and cross-linked NCs.[49,50] The necked NC dimers exhibit less pronounced electronic confinement and thus have a smaller band gap.[48] In this picture, an electron trap stems from the energy mismatch of the lowest unoccupied electronic states between an NC dimer and the surrounding, non-necked NCs (Figure 4ii). Second, trap states can also originate from doped NCs (Figure 4iii).[51] Oxidation of an n-type doped NC (or reduction of a p-doped NC) shifts the electronic structure of that doped-NC with respect to its neighbors, creating an electron (or hole trap). This means that doping and ultimately free carrier generation are directly linked to detrimental trap state formation.

The insights into electronic structure in NC thin films have been enabled by careful and systemic experimental and computational investigations. While optical techniques such as (transient) absorption or photoluminescence spectroscopy can be extremely useful in understanding the spacing between electronic levels in NCs and carrier dynamics,[52] determination of electronic structure referenced to the vacuum level is particularly important in device engineering. We thus focus here on photoemission (or photoelectron) spectroscopy (PES), electrochemical voltammetry, and scanning tunneling spectroscopy (STS) for which features in the electronic structure can be reported versus vacuum level (Figure 5, top).

We focus here on photoemission (or photoelectron) spectroscopy, electrochemical voltammetry, and scanning tunneling spectroscopy for which features in the electronic structure can be reported versus vacuum level.

Ultraviolet photoelectron spectroscopy (UPS) uses radiation from gas discharge lines (typically, on the order of tens of electronvolts) to excite electrons from filled states.[53] Recording the number of electrons leaving the sample as a function of their kinetic energy enables one to map the electron density of states (DOS) in the valence band. In inverse photoelectron spectroscopy (IPES), electrons impinging on the sample fill unpopulated band states and lead to photon emission, which maps the energy levels of unoccupied electronic states (i.e., the conduction band DOS).[54] UPS and IPES have been applied to thin films (or monolayers) of NCs on conductive substrates (e.g., Au or conductive metal oxides) to measure, for example, the impact of size,[55] composition,[56] and ligand species.[17]

In electrochemical voltammetry, the potential at a working electrode (either in contact with solvated NCs or a deposited NC thin film) is changed relative to that of a reference electrode such that the Fermi level in the NC (thin film) changes. The resulting current associated with charge transfer into and out of the NCs (i.e., oxidation or reduction) can be associated with the density of available states at the given potential (Figure 5, bottom).[57] These measurements are ideally performed using a three-electrode setup, where the reference electrode enables the potentials to be converted to an energy level versus vacuum.[58,59] The NC film is in an inert electrolyte, where the salt ions migrate in the vicinity of the NC film in order to facilitate the charge transport to/from the NCs to the working electrode. Electrochemical voltammetry techniques are identified by the type of perturbation and include linear sweep voltammetry (single linear sweep), cyclic voltammetry (CV, cyclic linear sweeps),[60−64] electrochemical impedance spectroscopy (EIS, sinusoidal perturbation),[65,66] or differential pulse voltammetry (series of short voltage pulses).[67,68] They can be combined with optical excitation (spectroelectrochemistry) to gain further insight into (de)-population of states.[69−76] These approaches have been applied to solvated NCs and NC films to determine band onsets as a function of composition, size, composition, and ligand functionalizations.[77−79]

Electrochemical open-circuit potential (i.e., potential of zero net current flow between working and counter electrode) measurements (Figure 5, bottom) can be used to determine the Fermi level in an NC solid.[20] For this it is necessary to also

https://dx.doi.org/10.1021/acs.jpclett.0c01417
J. Phys. Chem. Lett. 2020, 11, 9255−9264

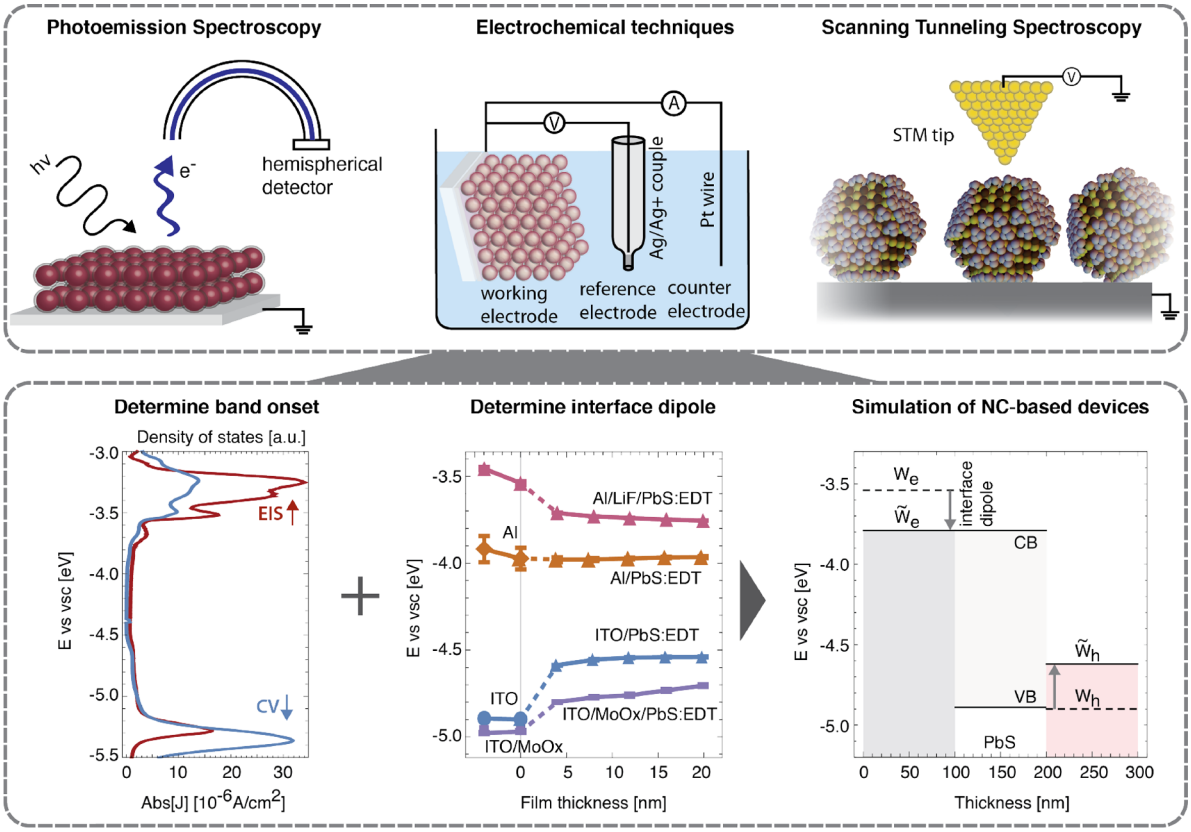

Figure 5. Experimental techniques to probe the electronic structure in NC thin films and roadmap toward an understanding of device performance. Top left: Schematic of an ultraviolet photoelectron spectroscopy setup. Top center: Working principle of an electrochemical setup in standard 3-electrode configuration. Reproduced from ref 57. Copyright 2018 American Chemical Society. Top right: Schematic of a scanning tunneling spectroscopy setup. Bottom: Depicted roadmap toward full understanding of the electronic structure in NC solids using electrochemical techniques. The energy position of band edge states can be assessed through energy-resolved electrochemical impedance spectroscopy (ER-EIS). Reproduced from ref 57. Copyright 2018 American Chemical Society. Open-circuit measurements can be used to determine both the Fermi level in NC thin films as well as interface dipoles at metal:NC contacts. Reproduced from ref 20. Copyright 2018 American Chemical Society. Together, these techniques quantify input parameters needed to facilitate device simulation. Reproduced from ref 21. Copyright 2019 AIP Publishing LLC.

use a redox couple (e.g., Fc/Fc+) to achieve a stable electrochemical potential in solution.

One advantage of electrochemical techniques is that they do not require ultrahigh vacuum (UHV) conditions. In fact, the same solvents utilized in the NC thin-film fabrication processes can sometimes be used as the electrochemical measurement environment,[20] enabling *in situ* monitoring of the electronic structure of NC thin films during their assembly.

Scanning tunneling spectroscopy (STS) can be used to assess the electronic DOS of individual NCs.[80] STS is performed by positioning the scanning probe close to the surface of either an isolated NC or a layer of NCs on a metallic substrate and recording the tunneling current between tip and thin film as a function of applied bias. The derivative of the tunneling current (dI/dV) is proportional to the DOS.[81] In this way, STS has been applied to measure the local electronic structure in PbS,[82,83] PbSe,[84,85] InAs,[81,86] and CdSe.[87−89] STS offers two unique aspects. First, it probes not only information about the electronic structure but also the topology of the film, enabling correlation between the physical characteristics of the NC and its structure. Second, it measures the electronic structure of individual NCs and not average values coming from an ensemble of nanocrystals. This allows investigation of the local variations in electronic structure, stemming for example from an NC size distribution.[84]

Photoelectron, electrochemical, and scanning probe measurements all have advantages and disadvantages in terms of sample preparation (e.g., smooth monolayers vs thin films tens of nanometers in thickness), measurement effort (e.g., equipment and sample environment required), and the information obtained (e.g., ensemble or local). However, when measuring the electronic structure in NC thin films, two aspects must always be considered: (i) charging and (ii) degradation.

In PES, the sample needs to be both conductive and grounded to avoid charging. This puts limits on the types of NC samples that can be measured and requires the impact of the work function of the substrate on the measured electronic structure of the NC to be considered. In PES, charging is observed as a shift and blurring of the spectra during the collection, and a potential bias or flood lamp can be used to confirm or mitigate the effects of charging. In STS and EC, charging is the fundamental working principle of the measurements. Changing the Fermi level leads to a rearrangement of charge carriers due to the (de)population of electronic states. In the case of NC oxidation or reduction, the whole electronic structure of the affected NC shifts to lower or higher energies, respectively. In PbS NC solids, these charging energies have been calculated to be up to 0.5 eV.[51] This has to be taken into consideration when STS or EC spectra are used to derive the electronic structure in NC solids.

https://dx.doi.org/10.1021/acs.jpclett.0c01417
J. Phys. Chem. Lett. 2020, 11, 9255−9264

Simultaneous probing of large NC ensembles as in the case of electrochemical (EC) techniques makes identification of individual states much more complicated[47,57] as charged and uncharged entities are mixed. We note that the ability to observe charging in STS and EC approaches should not be considered a shortcoming, but rather be leveraged to study NC electronic structure in the presence of charge.

Furthermore, all techniques can also potentially induce sample degradation. Both PES and STS typically involve inserting the sample into a high-vacuum environment. In PES, sputter cleaning of the film (if used) or the high-energy radiation can lead to physical or thermal degradation of the film. Sample degradation in electrochemical experiments can stem from solvent−sample interactions and/or the applied potential.[20] Polar solvents tend to lead to higher conductivity electrolytes (enabling shorter current transients with a potential perturbation), but can also etch materials. In general, sequential measurements reveal whether a certain technique can be regarded as noninvasive to a specific material set and thus be used as an *in situ* technique.

No matter which experimental technique is selected to map electronic structure, theory and computational models are often necessary to help understand and systematically fit the obtained data.[55,57]

Because electronic structure of an NC thin film is related to the electronic structure of the individual NC building blocks, we first describe the two categories of computational approaches to characterize the electronic structure of individual NCs isolated in vacuum (Figure 6): (i) top-down approaches based on the bulk band-structure of the NC material and (ii) large-scale density-functional theory (DFT) calculations on complete atomistic models of the NCs.

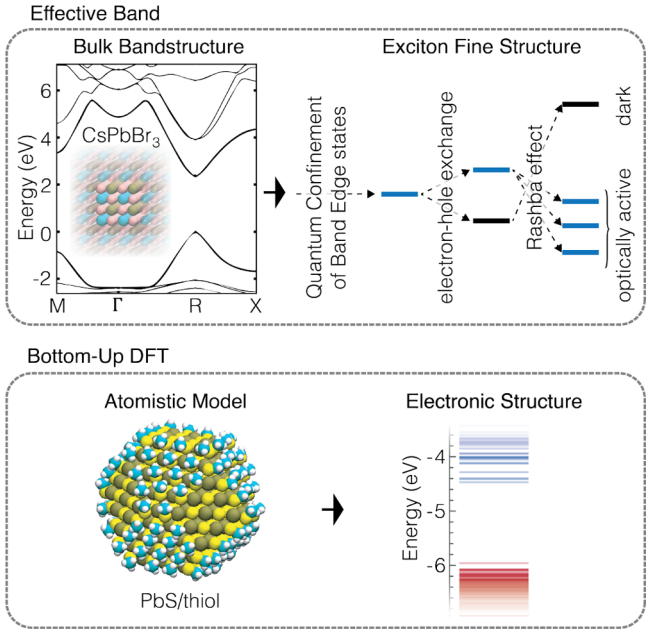

Figure 6. Computational methods to simulate electronic structure in nanocrystals. Top: Calculation of the bulk band-structure of $CsPbBr_3$ used to parametrize a multiband model in order to compute the exciton fine structure of $CsPbBr_3$ NCs. This approach can explain the experimental observation of an optically active triplet state as the lowest-energy transition in the NC. Reproduced from ref 95. Copyright 2018 Macmillan Publishers Limited. Bottom: Bottom-up atomistic DFT calculations can explicitly treat surface terminating ligands and directly provide the electronic structure. Reproduced from ref 104. Copyright 2018 American Chemical Society.

> The full potential of NC thin films will be reached with full understanding and control of the electronic structure of the individual NCs as well as their collective electronic structure when integrated into a thin film and ultimately into an entire device.

Top-down approaches begin with DFT bulk band-structure calculations of the material. By fitting to the bulk band-structures, tight-binding (TB) models can be parametrized for the material, after which, TB calculations can be performed on atomistic models of NCs.[90−92] Once parametrized, calculation of the electronic structure of an NC with TB is extremely fast, and this approach is suitable for studies in which the electronic structure of many different NCs needs to be computed (e.g., composition dependence of ternary NCs,[93] core−shell NCs in the presence of field[91]).

Bulk band structure results can also be employed in the parametrization of effective-mass, multiband models (EMMB). Compared to TB models, EMMB have the advantage that they can be readily amended with perturbative corrections, such as electron−hole exchange, lattice and NC shape asymmetry,[94] and spin−orbit coupling.[95] This renders EMMB approaches very powerful in determining the electronic fine-structure of NCs, right at the band gap.[96] For example, an EMMB model constructed for zinc-blende NCs was able to accurately reconstruct the exciton fine structure in CdSe NCs, identifying a weakly optically coupled lowest energy transition, or "dark exciton" for these NCs.[94] A model constructed for cesium−lead-halide perovskite NCs was able to provide an explanation for the experimentally observed optically bright lowest-energy transition in $CsPbBr_3$ NCs, which can result from a strong Rashba effect.[95]

Top-down approaches typically assume a significantly simplified physical structure of the NCs, ignoring their full atomistic complexity. In particular, charge compensating ligands and undercoordinated atoms on the surface of the NCs can impose complex NC shapes and lattice strains[97,98] and modify the bonding chemistry occurring at the interface.[99,100] Such effects can strongly impact the electronic structure of the NCs but cannot be readily investigated with top-down approaches. Fortunately, the efficiency of modern DFT codes[101,102] along with the increase in large-scale-computing resources has enabled the *ab initio* calculation of the electronic structure of systems of up to thousands of atoms. This allows the routine calculation of the electronic structure of NCs of up to ∼10 nm with their full atomic complexity, including ligands.[40,41,103−108] While these calculations provide highly accurate estimations of the single electron states over all energy scales, fine-structure detail is lost because of the absence of exciton exchange and the enormous cost of the inclusion of higher-order effects (e.g., spin orbit). Finally, at the cost of accuracy, hybrid schemes such as tight binding density functional theory (DFTB)[109] and mixed DFT/

https://dx.doi.org/10.1021/acs.jpclett.0c01417
J. Phys. Chem. Lett. 2020, 11, 9255−9264

molecular-mechanics[110] offer the possibility of treating much larger and complex systems, including, for example, solvent−NC interactions.

Further effort is required to link the electronic structure of individual NCs to the electronic structure of NC superlattices. The resulting quantum confined states of EMMB models can be used as a basis set in tight-binding models for the computation of the band-structure of NC thin films.[111] To date, direct bottom-up *ab initio* calculation of the electronic structure of NC thin films has remained impractical because of the high computational cost. However, in the case of weakly interacting NCs, the Hamiltonian of the NC thin film can be approximated as block diagonal, with each block corresponding to one NC within the superlattice, allowing tremendous computational savings.[51] Such a scheme enables the direct calculation of the electronic structure of the NC superlattice, including the full atomistic complexity of the superlattice.[51]

The full potential of NC thin films will be reached with full understanding and control of the electronic structure of the individual NCs as well as their collective electronic structure when integrated into a thin film and ultimately into an entire device. At each level, significant opportunities for further development exist.

At the level of individual NCs, recent work has shown the possibility of controlling the electronic structure of individual nanocrystals. Directional control of NC characteristics can be achieved already during synthesis by controlling NC surface and shape, for example through facet-selective epitaxy (Figure 7i).[90]

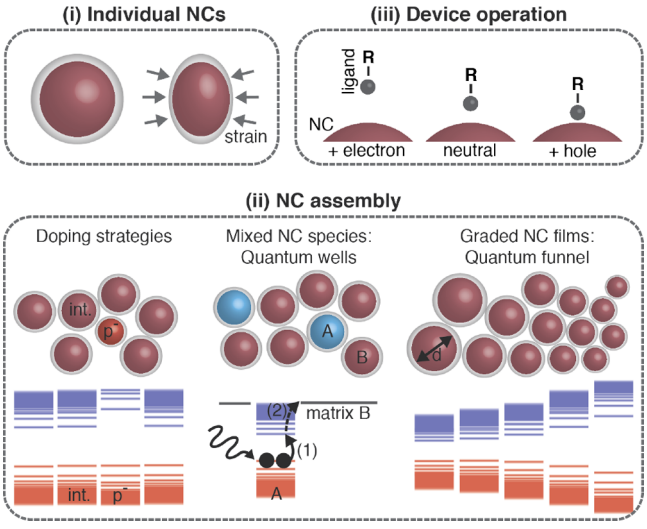

Figure 7. Opportunities for nanocrystal semiconductors. Understanding of electronic structure of NC-based semiconductors enables exploitation of their full potential by tuning (i) individual NCs through control of atomic positions and strain, (ii) their thin-film assembly (e.g., to induce doping postsynthesis or introduce quantum structuring by mixing NC species), and (iii) under device operation.

At the level of the NC thin film, substantial opportunities exist in using mixed NC species to create unique electronic structures (Figure 7i). When it comes to NC doping, we propose using individual NCs as donors or acceptors.[51] Such a structure can be realized by blending small amounts of doped NCs into a host system of intrinsic dots having a smaller band gap. This offers the potential to (i) eliminate deep level trap states and (ii) increase mobilities by several orders of magnitude through a reduction of the energetic barrier associated with the thermal release of the donor/acceptor charge.[51] This may have been already been realized by Urban et al., where mixing of Ag_2Te NCs with PbSe NCs of smaller band gap into superstructures was observed to increase the conductance by 2 orders of magnitude compared to lattices composed of the individual NC species.[112] Alteratively, tailored electronic structures within NC thin films can be achieved by spatially varying NC species. Mixing different NC species was used to generate quantum well structures,[33,113] and thin films assembled from NCs with progressively changing band gaps can give rise to quantum funnels with charge-carrier type preferred transport direction.[114]

> NC thin films are poised to become truly functional electronic solids offering unprecedented opportunities to leverage quantum effects within semiconductor thin films.

Because of electron−phonon coupling,[115−118] the electronic structure of a NC is not an immutable property but depends on the excitation state of the NC[119,120] and/or if an excess charge carrier is present on the NC.[51,121] At the device engineering level, a fundamental understanding of electron−phonon coupling and its role in carrier dynamics, such as intraband cooling,[122−125] charge transport, and exciton diffusion,[51,121,126] is therefore key to further improvement of NC semiconductors. For example, in the case of NC thin films fabricated with NCs in the strong quantum confined regime, charge carriers are localized on individual NCs forming polarons, with transport occurring through phonon-mediated polaron hopping,[51] while in larger NCs exhibiting weaker confinement, there is recent evidence suggesting carrier delocalization over multiple NCs.[127]

With progressively deeper understanding of electronic structure in semiconductors assembled from colloidal NCs and new opportunities emerging for controlling electronic structure at the level of the individual NCs to the device, NC thin films are poised to become truly functional electronic solids offering unprecedented opportunities to leverage quantum effects within semiconductor thin films.

AUTHOR INFORMATION

Corresponding Author

Vanessa Wood − *Department of Information Technology and Electrical Engineering, ETH Zurich, Zurich, Switzerland 8092;* orcid.org/0000-0001-6435-0227; Email: wood@iis.ee.ethz.ch

Authors

Sebastian Volk − *Department of Information Technology and Electrical Engineering, ETH Zurich, Zurich, Switzerland 8092*

Nuri Yazdani − *Department of Information Technology and Electrical Engineering, ETH Zurich, Zurich, Switzerland 8092*

Complete contact information is available at: https://pubs.acs.org/10.1021/acs.jpclett.0c01417

Notes

The authors declare no competing financial interest.

https://dx.doi.org/10.1021/acs.jpclett.0c01417
J. Phys. Chem. Lett. 2020, 11, 9255−9264

Biographies

Dr. Sebastian Volk received his M.Sc. in Physics with distinction from ETH Zürich in 2013 and his Ph.D. from ETH Zürich in 2020. He completed his doctoral research in the group of Vanessa Wood in the Department of Information Technology and Electrical Engineering, where he investigated the electronic structure of nanocrystal-based semiconductor thin films. His thesis focused on the development and combination of optoelectronic and electrochemical characterization techniques to derive an understanding of electronic midgap state formation in PbS nanocrystal solids.

Dr. Nuri Yazdani is a postdoctoral researcher in the group of Professor Vanessa Wood the Department of Information Technology and Electrical Engineering at ETH Zürich, focusing on experimental and computational understanding of phonons, electron−phonon coupling, and multiphonon-mediated charge carrier dynamics in nanocrystal quantum dots. He received his Ph.D. from ETH Zürich in 2017 and his M.Sc. in Engineering Physics from Simon Fraser University.

Professor Vanessa Wood received her M.Sc. and Ph.D. degrees in Electrical Engineering from the Massachusetts Institute of Technology in 2007 and 2010, respectively, where she worked in the research group of Prof. Vladimir Bulovic. Since 2011, she has held the chair in Materials and Device Engineering in the Department of Information Technology and Electrical Engineering at ETH Zürich. She received the Outstanding Young Investigator Award from the Materials Research Society in 2018. Since 2018, she also is head of the Department of Information Technology and Electrical Engineering.

REFERENCES

(1) Kagan, C. R.; Lifshitz, E.; Sargent, E. H.; Talapin, D. V. Building Devices from Colloidal Quantum Dots. *Science* **2016**, *353*, No. aac5523.

(2) Talapin, D. V.; Lee, J.-S.; Kovalenko, M. V.; Shevchenko, E. V. Prospects of Colloidal Nanocrystals for Electronic and Optoelectronic Applications. *Chem. Rev.* **2010**, *110*, 389−458.

(3) Kovalenko, M. V.; Manna, L.; Cabot, A.; Hens, Z.; Talapin, D. V.; Kagan, C. R.; Klimov, V. I.; Rogach, A. L.; Reiss, P.; Milliron, D. J.; et al. Prospects of Nanoscience with Nanocrystals. *ACS Nano* **2015**, *9*, 1012−1057.

(4) Voznyy, O.; Zhitomirsky, D.; Stadler, P.; Ning, Z.; Hoogland, S.; Sargent, E. H. A Charge-Orbital Balance Picture of Doping in Colloidal Quantum Dot Solids. *ACS Nano* **2012**, *6*, 8448−8455.

(5) Zarghami, M. H.; Liu, Y.; Gibbs, M.; Gebremichael, E.; Webster, C.; Law, M. P-Type PbSe and PbS Quantum Dot Solids Prepared with Short-Chain Acids and Diacids. *ACS Nano* **2010**, *4*, 2475−2485.

(6) Luther, J.; Law, M.; Song, Q.; Perkins, C.; et al. Structural, Optical, and Electrical Properties of Self-Assembled Films of PbSe Nanocrystals Treated with 1,2-Ethanedithiol. *ACS Nano* **2008**, *2*, 271−280.

(7) Osedach, T. P.; Zhao, N.; Andrew, T. L.; Brown, P. R.; Wanger, D. D.; Strasfeld, D. B.; Chang, L. Y.; Bawendi, M. G.; Bulovic, V. Bias-Stress Effect in 1,2-Ethanedithiol-Treated PbS Quantum Dot Field-Effect Transistors. *ACS Nano* **2012**, *6*, 3121−3127.

(8) Brus, L. E. A Simple Model for the Ionization Potential, Electron Affinity, and Aqueous Redox Potentials of Small Semiconductor Crystallites. *J. Chem. Phys.* **1983**, *79*, 5566−5571.

(9) Jasieniak, J.; Califano, M.; Watkins, S. E. Size-Dependent Valence and Conduction Band-Edge Energies of Semiconductor Nanocrystals. *ACS Nano* **2011**, *5*, 5888−5902.

(10) Gaponenko, S. V. *Optical Properties of Semiconductor Nanocrystals*; Cambridge University Press, 1998; p 106.

(11) Yarema, O.; Bozyigit, D.; Rousseau, I.; Nowack, L.; Yarema, M.; Heiss, W.; Wood, V. Highly Luminescent, Size- and Shape-Tunable Copper Indium Selenide Based Colloidal Nanocrystals. *Chem. Mater.* **2013**, *25*, 3753−3757.

(12) Yarema, O.; Yarema, M.; Lin, W. M. M.; Wood, V. Cu-In-Te and Ag-In-Te Colloidal Nanocrystals with Tunable Composition and Size. *Chem. Commun.* **2016**, *52*, 10878−10881.

(13) Yarema, O.; Yarema, M.; Bozyigit, D.; Lin, W. M. M.; Wood, V. Independent Composition and Size Control for Highly Luminescent Indium-Rich Silver Indium Selenide Nanocrystals. *ACS Nano* **2015**, *9*, 11134−11142.

(14) Protesescu, L.; Yakunin, S.; Bodnarchuk, M. I.; Krieg, F.; Caputo, R.; Hendon, C. H.; Yang, R. X.; Walsh, A.; Kovalenko, M. V. Nanocrystals of Cesium Lead Halide Perovskites ($CsPbX_3$, X = Cl, Br, and I): Novel Optoelectronic Materials Showing Bright Emission with Wide Color Gamut. *Nano Lett.* **2015**, *15*, 3692−3696.

(15) Jang, Y.; Shapiro, A.; Horani, F.; Abu-Hariri, A.; Lifshitz, E. Recent Advances in Colloidal IV-VI Core/Shell Heterostructured Nanocrystals. *J. Phys. Chem. C* **2018**, *122*, 13840−13847.

(16) Crisp, R. W.; Kroupa, D. M.; Marshall, A. R.; Miller, E. M.; Zhang, J.; Beard, M. C.; Luther, J. M. Metal Halide Solid-State Surface Treatment for High Efficiency PbS and PbSe QD Solar Cells. *Sci. Rep.* **2015**, *5*, 9945.

(17) Brown, P. R.; Kim, D.; Lunt, R. R.; Zhao, N.; Bawendi, M. G.; Grossman, J. C.; Bulović, V. Energy Level Modification in Lead Sulfide Quantum Dot Thin Films through Ligand Exchange. *ACS Nano* **2014**, *8*, 5863−5872.

(18) Kroupa, D. M.; Vörös, M.; Brawand, N. P.; McNichols, B. W.; Miller, E. M.; Gu, J.; Nozik, A. J.; Sellinger, A.; Galli, G.; Beard, M. C. Tuning Colloidal Quantum Dot Band Edge Positions through Solution-Phase Surface Chemistry Modification. *Nat. Commun.* **2017**, *8*, 15257.

(19) Santra, P. K.; Palmstrom, A. F.; Tanskanen, J. T.; Yang, N.; Bent, S. F. Improving Performance in Colloidal Quantum Dot Solar Cells by Tuning Band Alignment through Surface Dipole Moments. *J. Phys. Chem. C* **2015**, *119*, 2996−3005.

(20) Volk, S.; Yazdani, N.; Yarema, O.; Yarema, M.; Bozyigit, D.; Wood, V. In Situ Measurement and Control of the Fermi Level in Colloidal Nanocrystal Thin Films during Their Fabrication. *J. Phys. Chem. Lett.* **2018**, *9*, 7165−7172.

(21) Lin, W.; Yazdani, N.; Yarema, O.; Volk, S.; Yarema, M.; Kirchartz, T.; Wood, V. Simulating Nanocrystal-Based Solar Cells: A Lead Sulfide Case Study. *J. Chem. Phys.* **2019**, *151*, 241104.

(22) Sluydts, M.; De Nolf, K.; Van Speybroeck, V.; Cottenier, S.; Hens, Z. Ligand Addition Energies and the Stoichiometry of Colloidal Nanocrystals. *ACS Nano* **2016**, *10*, 1462−1474.

(23) Zhang, J.; Di, Q.; Liu, J.; Bai, B.; Liu, J.; Xu, M.; Liu, J. Heterovalent Doping in Colloidal Semiconductor Nanocrystals: Cation-Exchange-Enabled New Accesses to Tuning Dopant Luminescence and Electronic Impurities. *J. Phys. Chem. Lett.* **2017**, *8*, 4943−4953.

(24) Buonsanti, R.; Milliron, D. J. Chemistry of Doped Colloidal Nanocrystals. *Chem. Mater.* **2013**, *25*, 1305−1317.

(25) Luther, J. M.; Pietryga, J. M. Stoichiometry Control in Quantum Dots: A Viable Analog to Impurity Doping of Bulk Materials. *ACS Nano* **2013**, *7*, 1845−1849.

(26) Kim, D.; Kim, D. H.; Lee, J. H.; Grossman, J. C. Impact of Stoichiometry on the Electronic Structure of PbS Quantum Dots. *Phys. Rev. Lett.* **2013**, *110*, 196802.

(27) Wang, H.; Butler, D. J.; Straus, D. B.; Oh, N.; Wu, F.; Guo, J.; Xue, K.; Lee, J. D.; Murray, C. B.; Kagan, C. R. Air-Stable $CuInSe_2$ Nanocrystal Transistors and Circuits via Post-Deposition Cation Exchange. *ACS Nano* **2019**, *13*, 2324−2333.

(28) Ibáñez, M.; Hasler, R.; Liu, Y.; Dobrozhan, O.; Nazarenko, O.; Cadavid, D.; Cabot, A.; Kovalenko, M. V. Tuning P-Type Transport in Bottom-Up-Engineered Nanocrystalline Pb Chalcogenides Using Alkali Metal Chalcogenides as Capping Ligands. *Chem. Mater.* **2017**, *29*, 7093−7097.

(29) Kagan, C. R. Flexible Colloidal Nanocrystal Electronics. *Chem. Soc. Rev.* **2019**, *48*, 1626−1641.

(30) Kroupa, D. M.; Hughes, B. K.; Miller, E. M.; Moore, D. T.; Anderson, N. C.; Chernomordik, B. D.; Nozik, A. J.; Beard, M. C.

https://dx.doi.org/10.1021/acs.jpclett.0c01417
J. Phys. Chem. Lett. 2020, 11, 9255−9264

Synthesis and Spectroscopy of Silver-Doped PbSe Quantum Dots. *J. Am. Chem. Soc.* **2017**, *139*, 10382−10394.
(31) Stavrinadis, A.; Rath, A. K.; García De Arquer, F. P.; Diedenhofen, S. L.; Magén, C.; Martinez, L.; So, D.; Konstantatos, G. Heterovalent Cation Substitutional Doping for Quantum Dot Homojunction Solar Cells. *Nat. Commun.* **2013**, *4*, 2981.
(32) Papagiorgis, P.; Stavrinadis, A.; Othonos, A.; Konstantatos, G.; Itskos, G. The Influence of Doping on the Optoelectronic Properties of PbS Colloidal Quantum Dot Solids. *Sci. Rep.* **2016**, *6*, 18735.
(33) Yang, H.; Wong, E.; Zhao, T.; Lee, J. D.; Xin, H. L.; Chi, M.; Fleury, B.; Tang, H.-Y.; Gaulding, E. A.; Kagan, C. R.; et al. Charge Transport Modulation in PbSe Nanocrystal Solids by Au_xAg_{1-x} Nanoparticle Doping. *ACS Nano* **2018**, *12*, 9091−9100.
(34) Cargnello, M.; Johnston-Peck, A. C.; Diroll, B. T.; Wong, E.; Datta, B.; Damodhar, D.; Doan-Nguyen, V. V. T.; Herzing, A. A.; Kagan, C. R.; Murray, C. B. Substitutional Doping in Nanocrystal Superlattices. *Nature* **2015**, *524*, 450−453.
(35) Bozyigit, D.; Volk, S.; Yarema, O.; Wood, V. Quantification of Deep Traps in Nanocrystal Solids, Their Electronic Properties, and Their Influence on Device Behavior. *Nano Lett.* **2013**, *13*, 5284−5288.
(36) Bozyigit, D.; Lin, W. M. M.; Yazdani, N.; Yarema, O.; Wood, V. A Quantitative Model for Charge Carrier Transport, Trapping and Recombination in Nanocrystal-Based Solar Cells. *Nat. Commun.* **2015**, *6*, 6180.
(37) Nagpal, P.; Klimov, V. I. Role of Mid-Gap States in Charge Transport and Photoconductivity in Semiconductor Nanocrystal Films. *Nat. Commun.* **2011**, *2*, 486.
(38) Yoon, W.; Boercker, J. E.; Lumb, M. P.; Placencia, D.; Foos, E. E.; Tischler, J. G. Enhanced Open-Circuit Voltage of PbS Nanocrystal Quantum Dot Solar Cells. *Sci. Rep.* **2013**, *3*, 2225.
(39) Luther, J. M.; Law, M.; Beard, M. C.; Song, Q.; Reese, M. O.; Ellingson, R. J.; Nozik, A. J. Schottky Solar Cells Based on Colloidal Nanocrystal Films. *Nano Lett.* **2008**, *8*, 3488−3492.
(40) Katsiev, K.; Ip, A. H.; Fischer, A.; Tanabe, I.; Zhang, X.; Kirmani, A. R.; Voznyy, O.; Rollny, L. R.; Chou, K. W.; Thon, S. M.; et al. The Complete In-Gap Electronic Structure of Colloidal Quantum Dot Solids and Its Correlation with Electronic Transport and Photovoltaic Performance. *Adv. Mater.* **2014**, *26*, 937−942.
(41) Houtepen, A. J.; Hens, Z.; Owen, J. S.; Infante, I. On the Origin of Surface Traps in Colloidal II-VI Semiconductor Nanocrystals. *Chem. Mater.* **2017**, *29*, 752−761.
(42) Ip, A. H.; Thon, S. M.; Hoogland, S.; Voznyy, O.; Zhitomirsky, D.; Debnath, R.; Levina, L.; Rollny, L. R.; Carey, G. H.; Fischer, A.; et al. Hybrid Passivated Colloidal Quantum Dot Solids. *Nat. Nanotechnol.* **2012**, *7*, 577−582.
(43) Giansante, C.; Infante, I. Surface Traps in Colloidal Quantum Dots: A Combined Experimental and Theoretical Perspective. *J. Phys. Chem. Lett.* **2017**, *8*, 5209−5215.
(44) Du Fossé, I.; Ten Brinck, S.; Infante, I.; Houtepen, A. J. Role of Surface Reduction in the Formation of Traps in N-Doped II-VI Semiconductor Nanocrystals: How to Charge without Reducing the Surface. *Chem. Mater.* **2019**, *31*, 4575−4583.
(45) Voznyy, O.; Thon, S. M.; Ip, A. H.; Sargent, E. H. Dynamic Trap Formation and Elimination in Colloidal Quantum Dots. *J. Phys. Chem. Lett.* **2013**, *4*, 987−992.
(46) Zherebetskyy, D.; Zhang, Y.; Salmeron, M.; Wang, L. W. Tolerance of Intrinsic Defects in PbS Quantum Dots. *J. Phys. Chem. Lett.* **2015**, *6*, 4711−4716.
(47) Volk, S.; Yazdani, N.; Yarema, O.; Yarema, M.; Wood, V. Dopants and Traps in Nanocrystal-Based Semiconductor Thin Films: Origins and Measurement of Electronic Midgap States. *ACS Appl. Electron. Mater.* **2020**, *2*, 398−404.
(48) Gilmore, R. H.; Liu, Y.; Shcherbakov-Wu, W.; Dahod, N.; Lee, E.; Weidman, M.; Li, H.; Jean, J.; Bulovic, V.; Willard, A.; et al. Epitaxial Dimers and Auger-Assisted De-Trapping in PbS Quantum Dot Solids. *Matter* **2019**, *1*, 250−265.
(49) Hughes, B. K.; Ruddy, D. A.; Blackburn, J. L.; Smith, D. K.; Bergren, M. R.; Nozik, A. J.; Johnson, J. C.; Beard, M. C. Control of PbSe Quantum Dot Surface Chemistry and Photophysics Using an Alkylselenide Ligand. *ACS Nano* **2012**, *6*, 5498−5506.
(50) Evers, W. H.; Goris, B.; Bals, S.; Casavola, M.; De Graaf, J.; van Roij, R.; Dijkstra, M.; Vanmaekelbergh, D. Low-Dimensional Semiconductor Superlattices Formed by Geometric Control over Nanocrystal Attachment. *Nano Lett.* **2013**, *13*, 2317−2323.
(51) Yazdani, N.; Andermatt, S.; Yarema, M.; Farto, V.; Bani-Hashemian, M. H.; Volk, S.; Lin, W. M. M.; Yarema, O.; Luisier, M.; Wood, V. Charge Transport in Semiconductors Assembled from Nanocrystal Quantum Dots. *Nat. Commun.* **2020**, *11*, 2852.
(52) Klimov, V. I. *Nanocrystal Quantum Dots*; CRC Press, 2004.
(53) Cahen, D.; Kahn, A. Electron Energetics at Surfaces and Interfaces: Concepts and Experiments. *Adv. Mater.* **2003**, *15*, 271−277.
(54) Woodruff, P. *Modern Techniques of Surface Science*; Cambridge University Press: Cambridge, 2016.
(55) Miller, E. M.; Kroupa, D. M.; Zhang, J.; Schulz, P.; Marshall, A. R.; Kahn, A.; Lany, S.; Luther, J. M.; Beard, M. C.; Perkins, C. L.; et al. Revisiting the Valence and Conduction Band Size Dependence of PbS Quantum Dot Thin Films. *ACS Nano* **2016**, *10*, 3302−3311.
(56) Wood, V.; Panzer, M. J.; Halpert, J. E.; Caruge, J. M.; Bawendi, M. G.; Bulović, V. Selection of Metal Oxide Charge Transport Layers for Colloidal Quantum Dot LEDs. *ACS Nano* **2009**, *3*, 3581−3586.
(57) Volk, S.; Yazdani, N.; Sanusoglu, E.; Yarema, O.; Yarema, M.; Wood, V. Measuring the Electronic Structure of Nanocrystal Thin Films Using Energy-Resolved Electrochemical Impedance Spectroscopy. *J. Phys. Chem. Lett.* **2018**, *9*, 1384−1392.
(58) Trasatti, S. The "Absolute" Electrode Potential-the End of the Story. *Electrochim. Acta* **1990**, *35*, 269−271.
(59) Trasatti, S. The Absolute Electrode Potential: An Explanatory Note. *Pure Appl. Chem.* **1986**, *58*, 955−966.
(60) Liu, J.; Yang, W.; Li, Y.; Fan, L.; Li, Y. Electrochemical Studies of the Effects of the Size, Ligand and Composition on the Band Structures of CdSe, CdTe and Their Alloy Nanocrystals. *Phys. Chem. Chem. Phys.* **2014**, *16*, 4778−4788.
(61) Haram, S. K.; Quinn, B. M.; Bard, A. J. Electrochemistry of CdS Nanoparticles: A Correlation between Optical and Electrochemical Band Gaps. *J. Am. Chem. Soc.* **2001**, *123*, 8860−8861.
(62) Dissanayake, D. M. N. M.; Lutz, T.; Curry, R. J.; Silva, S. R. P. Measurement and Validation of PbS Nanocrystal Energy Levels. *Appl. Phys. Lett.* **2008**, *93*, 043501.
(63) Kucur, E.; Riegler, J.; Urban, G. A.; Nann, T. Determination of Quantum Confinement in CdSe Nanocrystals by Cyclic Voltammetry. *J. Chem. Phys.* **2003**, *119*, 2333−2337.
(64) Ning, Z.; Voznyy, O.; Pan, J.; Hoogland, S.; Adinolfi, V.; Xu, J.; Li, M.; Kirmani, A. R.; Sun, J.-P.; Minor, J.; et al. Air-Stable n-Type Colloidal Quantum Dot Solids. *Nat. Mater.* **2014**, *13*, 822−828.
(65) Bisquert, J.; Fabregat-Santiago, F.; Mora-Seró, I.; Garcia-Belmonte, G.; Barea, E. M.; Palomares, E. A Review of Recent Results on Electrochemical Determination of the Density of Electronic States of Nanostructured Metal-Oxide Semiconductors and Organic Hole Conductors. *Inorg. Chim. Acta* **2008**, *361*, 684−698.
(66) Wang, H.; Wang, Y.; He, B.; Li, W.; Sulaman, M.; Xu, J.; Yang, S.; Tang, Y.; Zou, B. Charge Carrier Conduction Mechanism in PbS Quantum Dot Solar Cells: Electrochemical Impedance Spectroscopy Study. *ACS Appl. Mater. Interfaces* **2016**, *8*, 18526−18533.
(67) Sobrova, P.; Ryvolova, M.; Hubalek, J.; Adam, V.; Kizek, R. Voltammetry as a Tool for Characterization of CdTe Quantum Dots. *Int. J. Mol. Sci.* **2013**, *14*, 13497−13510.
(68) Bloom, B. P.; Zhao, L.-B.; Wang, Y.; Waldeck, D. H.; Liu, R.; Zhang, P.; Beratan, D. N. Ligand-Induced Changes in the Characteristic Size-Dependent Electronic Energies of CdSe Nanocrystals. *J. Phys. Chem. C* **2013**, *117*, 22401−22411.
(69) Boehme, S. C.; Wang, H.; Siebbeles, L. D. a; Vanmaekelbergh, D.; Houtepen, A. J. Electrochemical Charging of CdSe Quantum Dot Films: Dependence on Void Size and Counterion Proximity. *ACS Nano* **2013**, *7*, 2500−2508.
(70) Boehme, S. C.; Walvis, T. A.; Infante, I.; Grozema, F. C.; Vanmaekelbergh, D.; Siebbeles, L. D. a; Houtepen, A. J. Electro-

https://dx.doi.org/10.1021/acs.jpclett.0c01417
J. Phys. Chem. Lett. 2020, 11, 9255−9264

chemical Control over Photoinduced Electron Transfer and Trapping in CdSe-CdTe Quantum-Dot Solids. *ACS Nano* **2014**, *8*, 7067−7077.
(71) Wang, C.; Shim, M.; Guyot-Sionnest, P. Electrochromic Nanocrystal Quantum Dots. *Science* **2001**, *291*, 2390−2392.
(72) Guyot-Sionnest, P.; Wang, C. Fast Voltammetric and Electrochromic Response of Semiconductor Nanocrystal Thin Films. *J. Phys. Chem. B* **2003**, *107*, 7355−7359.
(73) Spittel, D.; Poppe, J.; Meerbach, C.; Ziegler, C.; Hickey, S. G.; Eychmüller, A. Absolute Energy Level Positions in CdSe Nanostructures from Potential-Modulated Absorption Spectroscopy (EMAS). *ACS Nano* **2017**, *11*, 12174−12184.
(74) Wehrenberg, B. L.; Yu, D.; Ma, J.; Guyot-Sionnest, P. Conduction in Charged PbSe Nanocrystal Films. *J. Phys. Chem. B* **2005**, *109*, 20192−20199.
(75) Wehrenberg, B. L.; Guyot-Sionnest, P. Electron and Hole Injection in PbSe Quantum Dot Films. *J. Am. Chem. Soc.* **2003**, *125*, 7806−7807.
(76) Liu, H.; Keuleyan, S.; Guyot-Sionnest, P. N- and p-Type HgTe Quantum Dot Films. *J. Phys. Chem. C* **2012**, *116*, 1344−1349.
(77) Soreni-Harari, M.; Yaacobi-Gross, N.; Steiner, D.; Aharoni, A.; Banin, U.; Millo, O.; Tessler, N. Tuning Energetic Levels in Nanocrystal Quantum Dots through Surface Manipulations. *Nano Lett.* **2008**, *8*, 678−684.
(78) Querner, C.; Reiss, P.; Sadki, S.; Zagorska, M.; Pron, A. Size and Ligand Effects on the Electrochemical and Spectroelectrochemical Responses of CdSe Nanocrystals. *Phys. Chem. Chem. Phys.* **2005**, *7*, 3204−3209.
(79) Aldakov, D.; Querner, C.; Kervella, Y.; Jousselme, B.; Demadrille, R.; Rossitto, E.; Reiss, P.; Pron, A. Oligothiophene-Functionalized CdSe Nanocrystals: Preparation and Electrochemical Properties. *Microchim. Acta* **2008**, *160*, 335−344.
(80) Hamann, D. R.; Tersoff, J. Theory and Application STM. *Phys. Rev. B: Condens. Matter Mater. Phys.* **1985**, *31*, 805.
(81) Banin, U.; Millo, O. Tunnelling and Optical Spectroscopy of Semiconductor Nanocrystals. *Annu. Rev. Phys. Chem.* **2003**, *54*, 465−492.
(82) Logar, M.; Xu, S.; Acharya, S.; Prinz, F. B. Variation of Energy Density of States in Quantum Dot Arrays Due to Interparticle Electronic Coupling. *Nano Lett.* **2015**, *15*, 1855−1860.
(83) Diaconescu, B.; Padilha, L. A.; Nagpal, P.; Swartzentruber, B. S.; Klimov, V. I. Measurement of Electronic States of PbS Nanocrystal Quantum Dots Using Scanning Tunneling Spectroscopy: The Role of Parity Selection Rules in Optical Absorption. *Phys. Rev. Lett.* **2013**, *110*, 127406.
(84) Liljeroth, P.; Jdira, L.; Overgaag, K.; Grandidier, B.; Speller, S.; Vanmaekelbergh, D. Can Scanning Tunnelling Spectroscopy Measure the Density of States of Semiconductor Quantum Dots? *Phys. Chem. Chem. Phys.* **2006**, *8*, 3845.
(85) Overgaag, K.; Liljeroth, P.; Grandidier, B.; Vanmaekelbergh, D. Scanning Tunneling Spectroscopy of Individual PbSe Quantum Dots and Molecular Aggregates Stabilized in an Inert Nanocrystal Matrix. *ACS Nano* **2008**, *2*, 600−606.
(86) Banin, U.; Cao, Y. W.; Katz, D.; Millo, O. Identification of Atomic-like Electronic States in Indium Arsenide Nanocrystal Quantum Dots. *Nature* **1999**, *400*, 542−544.
(87) Jdira, L.; Liljeroth, P.; Stoffels, E.; Vanmaekelbergh, D.; Speller, S. Size-Dependent Single-Particle Energy Levels and Interparticle Coulomb Interactions in CdSe Quantum Dots Measured by Scanning Tunneling Spectroscopy. *Phys. Rev. B: Condens. Matter Mater. Phys.* **2006**, *73*, 115305.
(88) Bakkers, E. P. A. M.; Hens, Z.; Zunger, A.; Franceschetti, A.; Kouwenhoven, L. P.; Gurevich, L.; Vanmaekelbergh, D. Shell-Tunneling Spectroscopy of the Single-Particle Energy Levels of Insulating Quantum Dots. *Nano Lett.* **2001**, *1*, 551−556.
(89) Steiner, D.; Dorfs, D.; Banin, U.; Sala, F. D.; Manna, L.; Millo, O. Determination of Band Offsets in Heterostructured Colloidal Nanorods Using Scanning Tunneling Spectroscopy. *Nano Lett.* **2008**, *8*, 2954−2958.
(90) Fan, F.; Voznyy, O.; Sabatini, R. P.; Bicanic, K. T.; Adachi, M. M.; McBride, J. R.; Reid, K. R.; Park, Y. S.; Li, X.; Jain, A.; et al. Continuous-Wave Lasing in Colloidal Quantum Dot Solids Enabled by Facet-Selective Epitaxy. *Nature* **2017**, *544*, 75−79.
(91) Bozyigit, D.; Yarema, O.; Wood, V. Origins of Low Quantum Efficiencies in Quantum Dot LEDs. *Adv. Funct. Mater.* **2013**, *23*, 3024−3029.
(92) Moreels, I.; Lambert, K.; Smeets, D.; De Muynck, D.; Nollet, T.; Martins, J. C.; Vanhaecke, F.; Vantomme, A.; Delerue, C.; Allan, G.; et al. Size-Dependent Optical Properties of Colloidal PbS Quantum Dots. *ACS Nano* **2009**, *3*, 3023−3030.
(93) Yarema, O.; Yarema, M.; Wood, V. Tuning the Composition of Multicomponent Semiconductor Nanocrystals: The Case of I-III-VI Materials. *Chem. Mater.* **2018**, *30*, 1446−1461.
(94) Efros, A. L.; Rosen, M.; Kuno, M.; Nirmal, M.; Norris, D.; Bawendi, M. Band-Edge Exciton in Quantum Dots of Semiconductors with a Degenerate Valence Band: Dark and Bright Exciton States. *Phys. Rev. B: Condens. Matter Mater. Phys.* **1996**, *54*, 4843−4856.
(95) Becker, M. A.; Vaxenburg, R.; Nedelcu, G.; Sercel, P. C.; Shabaev, A.; Mehl, M. J.; Michopoulos, J. G.; Lambrakos, S. G.; Bernstein, N.; Lyons, J. L.; et al. Bright Triplet Excitons in Caesium Lead Halide Perovskites. *Nature* **2018**, *553*, 189−193.
(96) Efros, A. L.; Rosen, M. The Electronic Structure of Semiconductor Nanocrystals. *Annu. Rev. Mater. Sci.* **2000**, *30*, 475−521.
(97) Kim, K.; Yoo, D.; Choi, H.; Tamang, S.; Ko, J. H.; Kim, S.; Kim, Y. H.; Jeong, S. Halide-Amine Co-Passivated Indium Phosphide Colloidal Quantum Dots in Tetrahedral Shape. *Angew. Chem., Int. Ed.* **2016**, *55*, 3714−3718.
(98) Zherebetskyy, D.; Scheele, M.; Zhang, Y.; Bronstein, N.; Thompson, C.; Britt, D.; Salmeron, M.; Alivisatos, P.; Wang, L.-W. Hydroxylation of the Surface of PbS Nanocrystals Passivated with Oleic Acid. (Suppl Mat). *Science* **2014**, *344*, 1380−1384.
(99) Boles, M. A.; Ling, D.; Hyeon, T.; Talapin, D. V. The Surface Science of Nanocrystals. *Nat. Mater.* **2016**, *15*, 141−153.
(100) Owen, J. The Coordination Chemistry of Nanocrystal Surfaces. *Science* **2015**, *347*, 615−616.
(101) Andermatt, S.; Cha, J.; Schiffmann, F.; VandeVondele, J. Combining Linear-Scaling DFT with Subsystem DFT in Born-Oppenheimer and Ehrenfest Molecular Dynamics Simulations: From Molecules to a Virus in Solution. *J. Chem. Theory Comput.* **2016**, *12*, 3214−3227.
(102) VandeVondele, J.; Hutter, J. Gaussian Basis Sets for Accurate Calculations on Molecular Systems in Gas and Condensed Phases. *J. Chem. Phys.* **2007**, *127*, 114105.
(103) Yazdani, N.; Nguyen-Thanh, T.; Yarema, M.; Lin, W. M. M.; Gao, R.; Yarema, O.; Bosak, A.; Wood, V. Measuring the Vibrational Density of States of Nanocrystal-Based Thin Films with Inelastic X-Ray Scattering. *J. Phys. Chem. Lett.* **2018**, *9*, 1561−1567.
(104) Yazdani, N.; Bozyigit, D.; Vuttivorakulchai, K.; Luisier, M.; Infante, I.; Wood, V. Tuning Electron-Phonon Interactions in Nanocrystals through Surface Termination. *Nano Lett.* **2018**, *18*, 2233−2242.
(105) Drijvers, E.; De Roo, J.; Martins, J. C.; Infante, I.; Hens, Z. Ligand Displacement Exposes Binding Site Heterogeneity on CdSe Nanocrystal Surfaces. *Chem. Mater.* **2018**, *30*, 1178−1186.
(106) Ten Brinck, S.; Infante, I. Surface Termination, Morphology, and Bright Photoluminescence of Cesium Lead Halide Perovskite Nanocrystals. *ACS Energy Lett.* **2016**, *1*, 1266−1272.
(107) Voznyy, O.; Mokkath, J. H.; Jain, A.; Sargent, E. H.; Schwingenschlögl, U. Computational Study of Magic-Size Cdse Clusters with Complementary Passivation by Carboxylic and Amine Ligands. *J. Phys. Chem. C* **2016**, *120*, 10015−10019.
(108) Voznyy, O.; Levina, L.; Fan, F.; Walters, G.; Fan, J. Z.; Kiani, A.; Ip, A. H.; Thon, S. M.; Proppe, A. H.; Liu, M.; et al. Origins of Stokes Shift in PbS Nanocrystals. *Nano Lett.* **2017**, *17*, 7191−7195.
(109) Kar, M.; Rajbanshi, B.; Sarkar, R.; Pal, S.; Sarkar, P. Periodically-Ordered One and Two Dimensional CdTe QD Super-

https://dx.doi.org/10.1021/acs.jpclett.0c01417
J. Phys. Chem. Lett. 2020, 11, 9255−9264

structures: A Path Forward in Photovoltaics. *Phys. Chem. Chem. Phys.* **2019**, *21*, 19391−19402.
(110) Deng, L.; Woo, T. K.; Cavallo, L.; Margl, P. M.; Ziegler, T. The Role of Bulky Substituents in Brookhart-Type Ni(II) Diimine Catalyzed Olefin Polymerization: A Combined Density Functional Theory and Molecular Mechanics Study. *J. Am. Chem. Soc.* **1997**, *119*, 6177−6186.
(111) Shabaev, A.; Efros, A. L.; Efros, A. L. Dark and Photo-Conductivity in Ordered Array of Nanocrystals. *Nano Lett.* **2013**, *13*, 5454−5461.
(112) Urban, J. J.; Talapin, D. V.; Shevchenko, E. V.; Kagan, C. R.; Murray, C. B. Synergism in Binary Nanocrystal Superlattices Leads to Enhanced P-Type Conductivity in Self-Assembled PbTe/Ag_2Te Thin Films. *Nat. Mater.* **2007**, *6*, 115−121.
(113) Sun, B.; Ouellette, O.; García de Arquer, F. P.; Voznyy, O.; Kim, Y.; Wei, M.; Proppe, A. H.; Saidaminov, M. I.; Xu, J.; Liu, M.; et al. Multibandgap Quantum Dot Ensembles for Solar-Matched Infrared Energy Harvesting. *Nat. Commun.* **2018**, *9*, 4003.
(114) Livache, C.; Martinez, B.; Goubet, N.; Gréboval, C.; Qu, J.; Chu, A.; Royer, S.; Ithurria, S.; Silly, M. G.; Dubertret, B.; et al. A Colloidal Quantum Dot Infrared Photodetector and Its Use for Intraband Detection. *Nat. Commun.* **2019**, *10*, 2125.
(115) Bozyigit, D.; Yazdani, N.; Yarema, M.; Yarema, O.; Lin, W. M. M.; Volk, S.; Vuttivorakulchai, K.; Luisier, M.; Juranyi, F.; Wood, V. Soft Surfaces of Nanomaterials Enable Strong Phonon Interactions. *Nature* **2016**, *531*, 618−622.
(116) Mack, T. G.; Jethi, L.; Kambhampati, P. Temperature Dependence of Emission Line Widths from Semiconductor Nanocrystals Reveals Vibronic Contributions to Line Broadening Processes. *J. Phys. Chem. C* **2017**, *121*, 28537.
(117) Kelley, A. M. Exciton-Optical Phonon Coupling in II-VI Semiconductor Nanocrystals. *J. Chem. Phys.* **2019**, *151*, 140901.
(118) Liu, A.; Almeida, D. B.; Bae, W. K.; Padilha, L. A.; Cundiff, S. T. Non-Markovian Exciton-Phonon Interactions in Core-Shell Colloidal Quantum Dots at Femtosecond Timescales. *Phys. Rev. Lett.* **2019**, *123*, 057403.
(119) Seiler, H.; Palato, S.; Sonnichsen, C.; Baker, H.; Socie, E.; Strandell, D. P.; Kambhampati, P. Two-Dimensional Electronic Spectroscopy Reveals Liquid-like Lineshape Dynamics in CsPbI3 Perovskite Nanocrystals. *Nat. Commun.* **2019**, *10*, 4962.
(120) Yazdani, N.; Volk, S.; Yarema, O.; Yarema, M.; Wood, V. Size, Ligand, and Defect-Dependent Electron-Phonon Coupling in Chalcogenide and Perovskite Nanocrystals and Its Impact on Luminescence Line Widths. *ACS Photonics* **2020**, *7*, 1088−1095.
(121) Chu, I.-H.; Radulaski, M.; Vukmirovic, N.; Cheng, H.-P.; Wang, L.-W. Charge Transport in a Quantum Dot Supercrystal. *J. Phys. Chem. C* **2011**, *115*, 21409−21415.
(122) Boehme, S. C.; Brinck, S. t; Maes, J.; Yazdani, N.; Zapata, F.; Chen, K.; Wood, V.; Hodgkiss, J. M.; Hens, Z.; Geiregat, P.; et al. Phonon-Mediated and Weakly Size-Dependent Electron and Hole Cooling in $CsPbBr_3$ Nanocrystals Revealed by Atomistic Simulations and Ultrafast Spectroscopy. *Nano Lett.* **2020**, *20*, 1819−1829.
(123) Kilina, S. V.; Kilin, D. S.; Prezhdo, V. V.; Prezhdo, O. V. Theoretical Study of Electron-Phonon Relaxation in PbSe and CdSe Quantum Dots: Evidence for Phonon Memory. *J. Phys. Chem. C* **2011**, *115*, 21641−21651.
(124) Spoor, F. C. M.; Kunneman, L. T.; Evers, W. H.; Renaud, N.; Grozema, F. C.; Houtepen, A. J.; Siebbeles, L. D. A. Hole Cooling Is Much Faster than Electron Cooling in PbSe Quantum Dots. *ACS Nano* **2016**, *10*, 695−703.
(125) Diroll, B. T.; Schaller, R. D. Intraband Cooling in All-Inorganic and Hybrid Organic-Inorganic Perovskite Nanocrystals. *Adv. Funct. Mater.* **2019**, *29*, 1901725.
(126) Gilmore, R. H.; Winslow, S. W.; Lee, E. M. Y.; Ashner, M. N.; Yager, K. G.; Willard, A. P.; Tisdale, W. A. Inverse Temperature Dependence of Charge Carrier Hopping in Quantum Dot Solids. *ACS Nano* **2018**, *12*, 7741−7749.
(127) Lan, X.; Chen, M.; Hudson, M. H.; Kamysbayev, V.; Wang, Y.; Guyot-Sionnest, P.; Talapin, D. V. Quantum Dot Solids Showing State-Resolved Band-like Transport. *Nat. Mater.* **2020**, *19*, 323−329.
(128) Oh, S. J.; Berry, N. E.; Choi, J. H.; Gaulding, E. A.; Lin, H.; Paik, T.; Diroll, B. T.; Muramoto, S.; Murray, C. B.; Kagan, C. R. Designing High-Performance PbS and PbSe Nanocrystal Electronic Devices through Stepwise, Post-Synthesis, Colloidal Atomic Layer Deposition. *Nano Lett.* **2014**, *14*, 1559−1566.

https://dx.doi.org/10.1021/acs.jpclett.0c01417
J. Phys. Chem. Lett. 2020, 11, 9255−9264